The development of high performance hybrid joints between epoxy composites and PEEK/PPS composites

The mode-II and mix mode-I/II fracture behaviour

Quan, Dong; Zhao, Guoqun; Wang, Guilong; Alderliesten, René

DOI
10.1016/j.compstruct.2022.115638

Publication date
2022

Document Version
Final published version

Published in
Composite Structures

Composite Structures 292 (2022) 115638

Contents lists available at ScienceDirect

Composite Structures

journal homepage: www.elsevier.com/locate/compstruct

The development of high performance hybrid joints between epoxy composites and PEEK/PPS composites: The mode-II and mix mode-I/II fracture behaviour

Dong Quan [a], Guoqun Zhao [a,*], Guilong Wang [a], René Alderliesten [b]

[a] Key Laboratory for Liquid–Solid Structural Evolution and Processing of Materials (Ministry of Education), Shandong University, China
[b] Structural Integrity & Composites Group, Delft University of Technology, Netherlands

ARTICLE INFO

Keywords:
Hybrid composite joints
Surface treatment
Co-bond joining
Mode-II and mix mode-I/II fracture

ABSTRACT

The development of effective methods for the bonding of Poly-etherether-ketone (PEEK) and Polyphenylene-sulphide (PPS) composites to thermoset composites is appealing to expand their applications in aerospace industry. Herein, the surfaces of PEEK and PPS composites were treated by a high-power UV-irradiation technique for 6 s, that proved to significantly improve their intrinsically low surface activities. Carbon fibre reinforced epoxy composites were then directly cured onto the PEEK and PPS composites with or without an aerospace film adhesive at the joining interfaces. The mode-II and mix mode-I/II fracture behaviour of the hybrid joints were studied using an end notched flexural test and a fixed-ratio mixed-mode test, respectively. It was observed that the failure of the hybrid joints without adhesives mainly took place at the joining interfaces. In this case, the lack of resins at the fracture plane resulted in relatively low fracture toughness. Encouragingly, a cohesive failure was observed for the hybrid joints with adhesives in all the cases, owing to the enhanced adhesion between the adhesive and the PEEK/PPS composites upon the UV-treatment. This phenomenon indicated that optimal fracture resistance of the hybrid adhesive joints was obtained for the given material systems.

1. Introduction

Advanced thermoplastic composites, including Poly-etherether-ketone (PEEK) and Polyphenylene-sulphide (PPS) composites, offer many significant advantages over their thermoset counterparts, including high fracture toughness and impact resistance, excellent thermal resistance, good reformability and recyclability, short manufacturing process and infinite storage times. Accordingly, they have been increasingly used in aerospace industry by replacing the thermoset composites and metals over the last decade [1,2]. Moreover, the aerospace industry keeps putting more and more attention on the development of key structural components based on PEEK and PPS composites. For example, thousands of PEEK composite clips are used to join the epoxy composite spars to the epoxy composite skins of the fuselage in the A350 and Boeing 787 aircraft. Additionally, the 'wing of the future' project leaded by Airbus has developed a new generation aircraft wing consisting of a thermoset composite skin and thermoplastic composite spars and ribs [3].

Along with the combining usage of components based on advanced thermoplastic composites and thermoset composites in the aircrafts, the development of effective joining methods for their assembly becomes a foremost challenge facing by the researchers and engineers. Mechanical fastening [4,5] and adhesive bonding [6,7] are currently the main joining techniques for aircraft assembly, while welding (infusion bonding) has also attracted considerable attention for the joining of thermoplastic composites [8,9]. Among them, mechanical fastening using screws, rivets, bolts etc. is currently the dominating method for joining aerospace load-bearing structures. However, it is not considered as an ideal choice for composite materials due to the requirement of drilling holes and using heavy metal fasteners. Welding is another option for the joining of thermoplastic composites, and it proves to produce joints with good structural integrity with little surface preparation and short assembling time being needed. Nevertheless, it is not applicable for the joining of thermoset composites. Adhesive bonding offers the possibility of making light-weight constructions, the ability to join any pair of dissimilar materials with a relatively uniform stress-distribution, and the possibility to seal the entire bonding area and hence to provide high joint strength and durability [10]. Accordingly,

* Corresponding author.
E-mail address: zhaogq@sdu.edu.cn (G. Zhao).

https://doi.org/10.1016/j.compstruct.2022.115638
Received 27 December 2021; Received in revised form 13 February 2022; Accepted 23 April 2022
Available online 30 April 2022

it is considered to be the most suitable joining method for thermoset composites and hybrid thermoplastic-to-thermoset composite joints.

There are two main shortcomings of adhesive bonding: firstly, it needs long curing cycle for the bonding process, in addition to the curing of the composites; and secondly, it requires extensive surface preparation, especially for the majority of thermoplastic composites that possessed inherently low surface energies [11,12]. Regarding the disadvantage of a long curing cycle, the concepts of co-cure or co-bond have already proved to effectively shorten the manufacturing process, in which the laminate curing and adhesive bonding are carried out in a single processing operation [13,14]. However, the development of efficient surface treatment methods for advanced thermoplastic composites is still appealing. In previous study [15], we proposed a high-power UV-irradiation technique to prepare the surfaces of carbon fibre reinforced PEEK and PPS composites for adhesive bonding. It has been demonstrated that this technique is a highly effective, eco-friendly and low-cost surface-treatment method for advanced thermoplastic composites. It can overcome many limitations of traditional surface treatment methods [15], such as acid etching [16,17], corona discharge [18,19], plasma treatment [20,21], and oxidising flame treatment [22,23]. In specific, hybrid composite joints were prepared by the direct cure of epoxy composites onto UV-treated PEEK and PPS composites in [15]. It was observed that applying a high-power UV-treatment to the PEEK and PPS composites for just 6 s considerably enhanced their adhesion with aerospace adhesives, and resulted in significantly improved lap-shear strength and mode-I fracture energies of the hybrid joints. Moreover, the failure mode of the adhesive joints had been transited from interface failure to either cohesive failure or substrate damage, which indicated a high structural integrity of the joints under the corresponding loading conditions.

While the previous work [15] focused on the lap-shear strength and mode-I fracture behaviour of the hybrid composite joints, this study investigated their mode-II and mix mode-I/II fracture behaviour, with an attempt to further understand their structural performance and failure behaviour. Herein, the same materials and manufacturing process as in [15] were used to manufacture hybrid joints between epoxy composites and PEEK/PPS composites, with and without film adhesives at the joining interfaces. The mode-II and mix mode-I/II fracture behaviour of the hybrid joints were studied using an end notched flexural (ENF) test and a fixed-ratio mixed-mode (FRMM) test, respectively. The fracture mechanisms of the adhesive joints were also investigated.

2. Experimental

2.1. Materials and sample preparation

The prepregs of carbon fibre reinforced PPS composite and carbon fibre reinforced PEEK composite were supplied by TenCate Advanced Composites, the Netherlands. They possessed the same carbon fibre reinforcements that were 5-harness satin weave fabrics. The carbon fibre reinforced epoxy composite was unidirectional prepreg, HexPly 8552-IM7-35%-134 from Hexcel. The epoxy adhesive used for co-bonding was FM300 from Solvay. This was an aerospace-grade film adhesive that was supported by a non-woven thermoplastic carrier.

Fig. 1 briefly summarises the processes for sample preparation. The PEEK and PPS composite panels were manufactured by the consolidation of a $[0/90]_{4S}$ layup in a hot-platen press (Joos LAP100) at 2 MPa and 400 °C (for PEEK composite) or 320 °C (for PPS composite) for 30 mins, as shown in Figs. 1 (a)–(b). The bonding surfaces of the PEEK and PPS composite panels were then treated by a high-power UV-irradiation technique for just 6 s, see Fig. 1 (c). The intensities of the UV spectral ranges applied onto the composite surfaces are presented in Table 1, that were measured using a UV Power Puck from EIT Inc., USA. This treatment procedure was inherited from the previous study [15], and it proved to be sufficient to improve the adhesion between the adhesive and the PEEK and PPS composites. After the surface treatment, 8 layers of unidirectional carbon fibre/epoxy prepreg were laid onto the UV-treated thermoplastic composite panels, with and without a layer of film adhesive placed at the bonding interface, as shown in Fig. 1 (d). A PTFE film with a thickness of 12.7 μm was also inserted at the bonding interface for the generation of a crack starter within the fracture specimens. The non-cured assembles of the hybrid joints were then sealed in a vacuum bag and placed in an autoclave for co-bonding, see Fig. 1 (e). The curing schedule was 180 °C and 0.4 MPa gauge pressure within the autoclave for 90 mins, and a 200 mbar vacuum pressure was also applied within the vacuum bag throughout the entire process. The cured composite joints were then machined into desired dimensions for the following fracture tests, as shown in Fig. 1 (f). Finally, specimens for the fracture tests of the hybrid composite joints with and without adhesive at the joining interface were obtained, as shown by the side-view images of the joints in Fig. 1 (g). The configurations of the composite joints were designed to ensure the bending stiffnesses of the PEEK and PPS composite substrates and the epoxy composite substrates were essentially the same. It is noteworthy that hybrid joints consisting of non-treated PEEK/PPS composite substrates were also prepared using the same process. However, they all failed during the cutting process due to the very poor adhesion at the interfaces between the adhesives and the PPS and PEEK composites. More detailed information about the materials and the sample preparation processes can be found in [15].

Table 1
The intensities of the UV spectral ranges applied onto the PEEK and PPS composite surfaces.

Items	Wave length (nm)	Intensity (mW/cm^2)
UVA	320–390	1546
UVB	280–320	343
UVC	250–260	51
UVV	395–445	1979

2.2. Testing and analysis

The mode-II fracture behaviour of the hybrid composite joints was studied using an end-notched flexural (ENF) test according to ASTM-D7905 [24]. Fig. 2 (a) shows the testing setup and sample dimensions of the ENF tests, that were carried out on a Zwick 10 kN testing machine at a constant displacement rate of 0.5 mm/min. Prior to the ENF tests, a precrack that was about 5 mm long was generated by loading the ENF specimens in an opening mode. The ENF tests were repeated for three times for each set. A compliance calibration method was used to determine the mode-II fracture energies of the hybrid composite joints [24]:

$$G_{IIC} = \frac{3mP_{max}^2 a_0^2}{2b} \quad (1)$$

where P_{max} is the maximum load, a_0 is the crack length used in the fracture test, b is specimen width and m is the compliance calibration coefficient, that was obtained by carrying the compliance calibration tests with a precrack length of 10 mm, 20 mm and 30 mm [24]. The compliance calibration tests were repeated on all the three samples for each set and then the average value of the compliance calibration coefficients was used for the energy calculations. It is worthy to mention that, prior to the testing, the location of the crack front within the ENF specimen was precisely determined by observing the side of the specimens using an optical microscope. During this process, the edge of the ENF specimen was slightly opened by inserting a razor blade for an easy observation of the crack tip.

A fixed-ratio mixed-mode (FRMM) test [25] was used to measure the mix mode-I/II fracture toughness of the hybrid joints, and the mode-mixity of mode-I/mode-II was 57%/43% [25]. A schematic of the sample dimensions and testing setup are shown in Fig. 2 (b). The tests

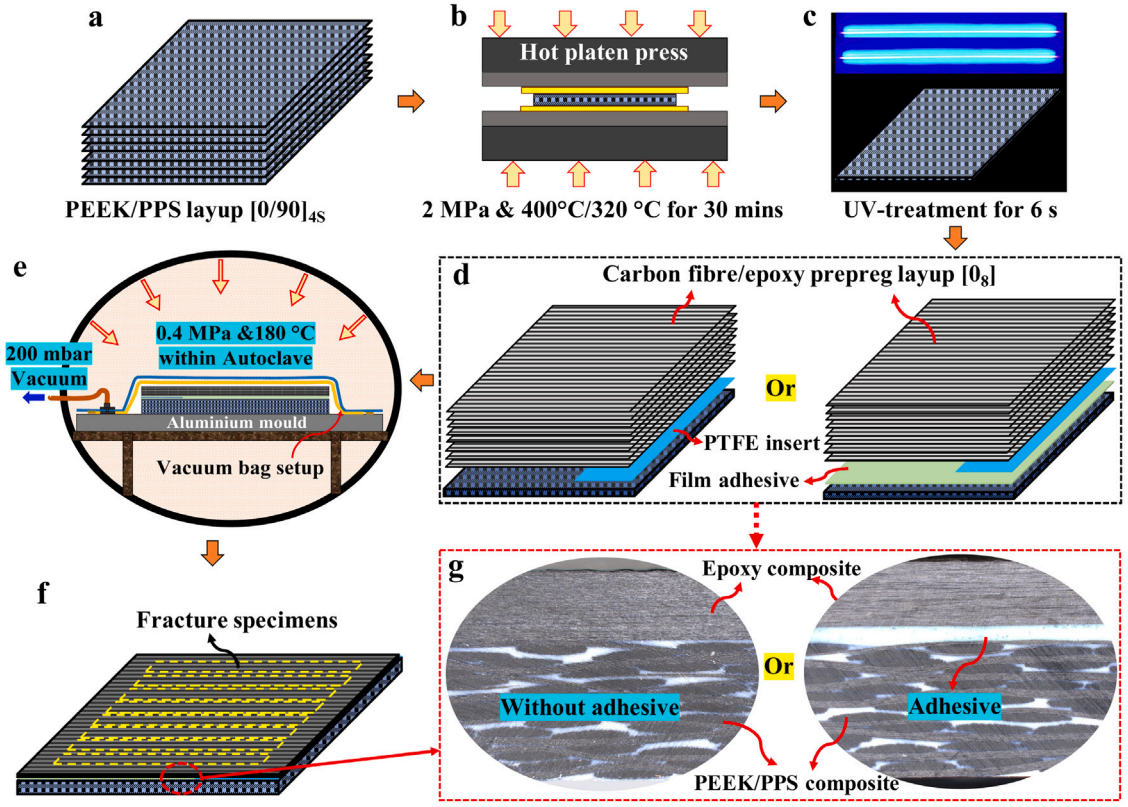

Fig. 1. Illustration of the sample preparation process.

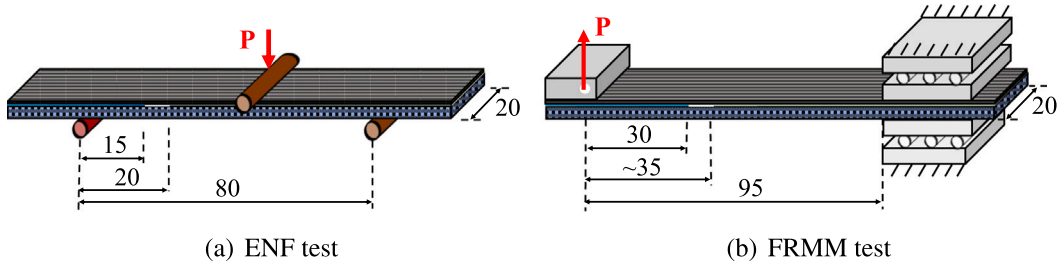

Fig. 2. Schematics of (a) the ENF test and (b) the FRMM test. The units for the values are in mm.

were carried out at a constant displacement rate of 2 mm/min using the Zwick 10 kN testing machine. An approximately 5 mm long precrack was also created by loading the FRMM specimens under an opening mode. During the FRMM tests, the length of the crack was monitored using a high resolution digital camera, and it was synchronised with the load and displacement measurements based on the start time of the test. The mix mode-I/II fracture energies corresponding to the measured crack lengths were then derived using a corrected beam theory [25], that is described as:

$$G_{I/IIC} = G_I + G_{II} \tag{2a}$$

$$G_I = \frac{3P^2(a+|\Delta_I|)^2}{b^2 E_f h^3} \cdot F \tag{2b}$$

$$G_{II} = \frac{9P^2(a+|\Delta_{II}|)^2}{4b^2 h^3 E_f} \cdot F \tag{2c}$$

where P is the load corresponding to the current crack length a, h is the thickness of the beam and E_f is the flexural modulus of the beam. F and Δ_I/Δ_{II} are the correction factors for large displacements and root rotation of the crack tip, respectively, as detailed in [26,27]. The average of all the calculated $G_{I/IIC}$ values for each hybrid joint specimen was determined as its mix mode-I/II fracture energy. Three replicable tests were carried out for each set.

The fracture surfaces of the ENF and FRMM specimens were imaged using a JSM-7500F scanning electron microscope (SEM) to investigate the fracture mechanisms of the hybrid joints. Prior to the SEM imaging, the surfaces of the samples were sputter coated with a layer of gold that possessed a thickness of approximately 5 nm.

3. Results and discussion

3.1. The mode-II fracture behaviour

The load versus displacement curves of the mode-II fracture tests for the hybrid composite joints are shown in Figs. 3(a) and (b). In Fig. 3 and the rest of this paper, PPS/EP represents the hybrid joints between the PPS composites and the epoxy (EP) composites without adhesives, while PPS/AD/EP indicates the corresponding hybrid joints with adhesives (AD). Similarly, PEEK/EP and PEEK/AD/PPS represent the hybrid joints between the epoxy composites and the PEEK composites without and with adhesives, respectively. From Figs. 3(a) and (b), it was observed that the hybrid joints bonded by the adhesives

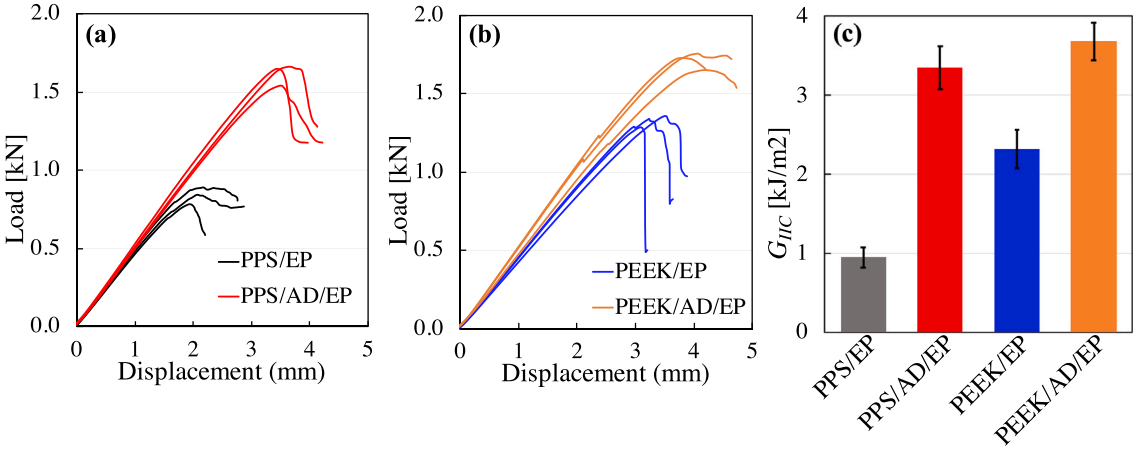

Fig. 3. Load versus displacement curves of the hybrid joints without adhesive layer (a) and with adhesive layers (b) from the ENF tests, and their corresponding mode-II fracture energies (c).

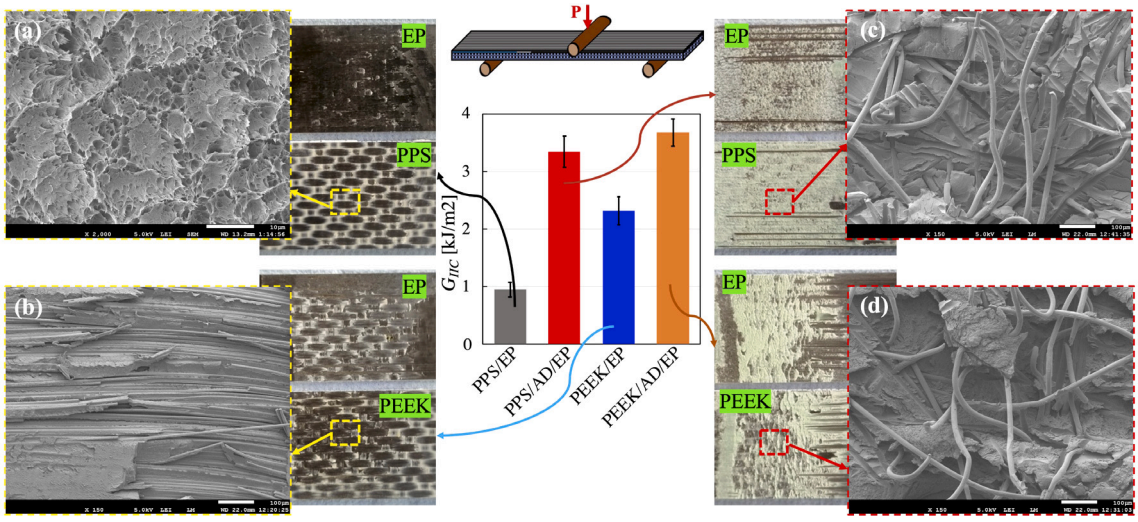

Fig. 4. Typical photographs and microscopy images of the mode-II fracture surfaces.

exhibited much higher failure loads than their counterparts without adhesives in both cases, indicating the necessity of using adhesives for effective bonding. Moreover, a comparison between Figs. 3 (a) and (b) showed that the failure loads of the PEEK/EP joints were much higher than that of the PPS/EP joints, while the failure loads of the PEEK/AD/EP joints were only slightly higher than that of the PPS/AD/EP joints. The corresponding mode-II fracture energies (G_{IIC}) of the hybrid adhesive joints are shown in Fig. 3 (c). Obviously, the fracture energies of the hybrid joints without adhesives were much lower than their counterparts with adhesives in both of the cases. In specific, a value of 0.96 kJ/m^2 was measured for G_{IIC} of the PPS/EP joints. The addition of an adhesive layer at the bonding interface significantly increased G_{IIC} to 3.35 kJ/m^2 of the PPS/AD/EP joints, corresponding to an increase of 249%. The value of G_{IIC} of the PEEK/EP joints was measured to be 2.32 kJ/m^2, that was 142% higher than that of the PPS/EP joints. Similarly, the PEEK/AD/EP joints possessed a much higher G_{IIC} (i.e. 3.68 kJ/m^2) than the PEEK/EP joints due to the presence of an adhesive layer at the interface.

To understand the fracture mechanisms of the hybrid joints and correlated them with the measured fracture energies, microscopy analysis was carried out on the mode-II fracture surfaces, as shown in Fig. 4. It should be noted that the colour of the FM300 adhesive was green after the curing. For the PPS/EP joints, the mode-II fracture failure mainly took place at the interface between the epoxy composites and the PPS composites. This fracture process was associated with the peeling-off of some PPS resins from the PPS composite substrates, that was evidenced by the presence of some white colour spots on the surfaces of the epoxy substrate, see the photograph for the PPS/EP joints in Fig. 4. Additionally, the inset image Fig. 4 (a) showed that extensive plastic deformation and failure took place to the matrix resin at the PPS substrate surface during the mode-II fracture process, indicating a good adhesion at the epoxy/PPS interface. Similar to the PPS/EP joints, the failure of the PEEK/EP joints also happened at the vicinity of the interface between the epoxy composites and the PEEK composites during the mode-II fracture process. However, evidence of intensive damage to the PEEK substrates was observed on the photograph for the PEEK/EP joints in Fig. 4, i.e. almost the entire surface of the epoxy substrate was covered with peeled-off PEEK resin and carbon fibres. The inset SEM image (b) further confirmed the presence of extensive carbon fibre breakage during the fracture process. These phenomena explained why the PEEK/EP joints exhibited a much better resistance to mode-II fracture than the PPS/EP joints, as shown in Fig. 3. For the adhesively bonded joints, a cohesive failure within the adhesive layers was observed for both of the PPS/AD/EP and PEEK/AD/EP joints, see the photographs on the right sides of Fig. 4. Moreover, the inset SEM images (c) and (d) in Fig. 4 show that the fracture surfaces were covered with numerous debonded fibres. These fibres were from the non-woven supporting carrier of the film adhesive. The extensive

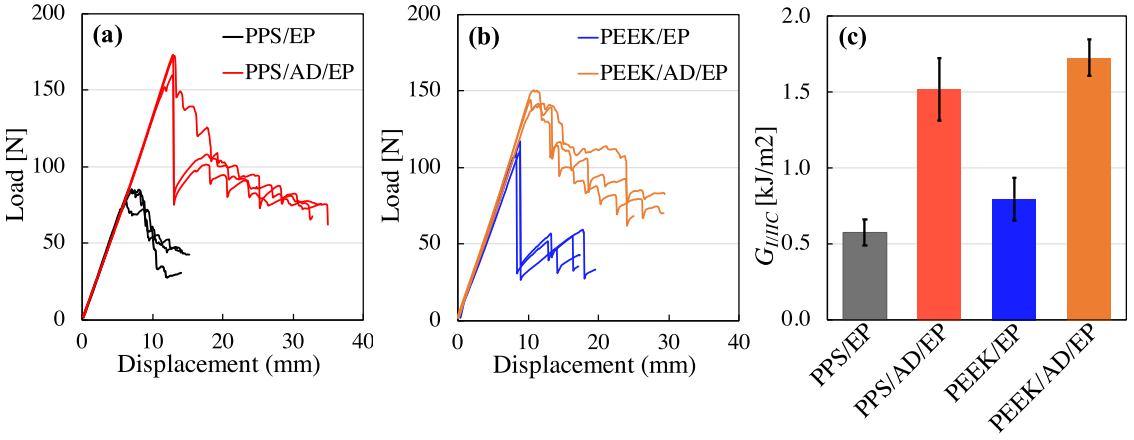

Fig. 5. Load versus displacement curves of the hybrid joints without adhesive layer (a) and with adhesive layers (b) from the FRMM tests, and their corresponding mix mode-I/II fracture energies (c).

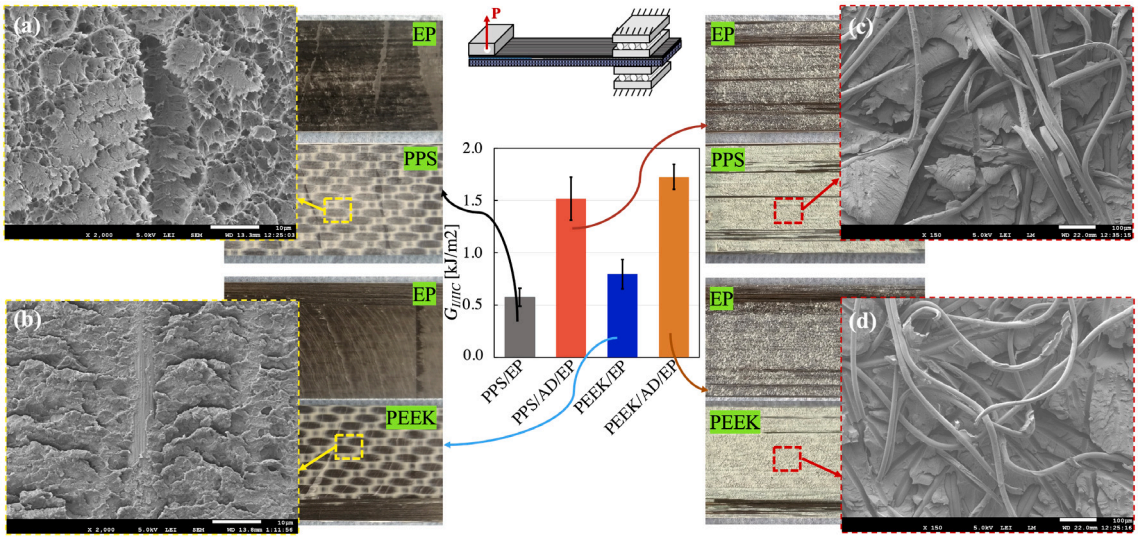

Fig. 6. Typical photographs and microscopy images of the mix mode-I/II fracture surfaces.

debonding and bridging mechanisms of the thermoplastic fibres proved to be highly effective for energy dissipation during the fracture process [28,29], and resulted in higher fracture energies of the PPS/AD/EP and PEEK/AD/EP joints when compare to their counterparts without adhesives, see Fig. 3.

3.2. The mix mode-I/II fracture behaviour

Figs. 5 (a) and (b) show the load versus displacement curves of the mix mode-I/II fracture tests of the hybrid composite joints, while Fig. 5 (c) presents the corresponding mix mode fracture energies. Overall, the failure loads of the mix mode-I/II fracture of the hybrid joints with adhesives were much higher than their counterparts without adhesives. This phenomenon was also observed for the mode-II fracture behaviour, and it further demonstrated that adding an adhesive layer at the joining interfaces was required to obtain a high bonding quality. Consequently, the fracture energies of the hybrid joints with adhesives were much higher when compared to the ones without adhesives, as shown in Fig. 5 (c). For example, a value of 1.52 kJ/m^2 was measured for the $G_{I/IIC}$ of the PPS/AD/EP joints, that was 162% higher than the $G_{I/IIC}$ value of the PPS/EP joints. Similar to the mode-II fracture, the PEEK/AD/EP joints possessed a highest $G_{I/IIC}$ of 1.73 kJ/m^2 in all the cases. This value was 116% higher than that of the PEEK/EP joints.

Fig. 6 shows typical photographs and SEM images of the mix mode-I/II fracture surfaces of the hybrid composite joints. The PPS/EP and PEEK/EP joints exhibited essentially the same fracture mechanisms, i.e. the crack propagation occurred at the joining interfaces in both cases. Moreover, the inset SEM images of Figs. 6 (a) and (b) present evidence of significant plastic deformation and failure of the matrix resins on the surfaces of the PEEK and PPS composites. These observations indicated a good adhesion between the epoxy composites and the PPS/PEEK composites. However, the lack of PPS/PEEK resins at the crack path lead to a small fracture damage zone ahead of the crack tip and resulted in the relatively low $G_{I/IIC}$ values. By taking a closer look at the photo of the fracture surfaces for the PEEK/EP joints, it was found that a bundle of carbon fibres delaminated from the epoxy substrates during the fracture process. This phenomenon resulted in a relatively higher $G_{I/IIC}$ of the PEEK/EP joints than the PPS/EP joints. For the adhesively bonded joints, both of the PPS/AD/EP and PEEK/AD/EP joints exhibited a cohesive failure within the adhesive layers. This was evidenced by the presence of green colour adhesives on both sides of the fracture surfaces, see the photographs for the PPS/AD/EP and

PEEK/AD/EP joints in Fig. 6. As already observed for the mode-II fracture, the cohesive failure was typically associated with debonding, bridging and breakage of thermoplastic supporting fibres, as shown by the inset SEM images (c) and (d). These mechanisms dissipated a good amount of energy during the mix mode-I/II fracture process of the adhesively bonded joints, and resulted in the relatively high fracture energies in Fig. 3.

4. Conclusions

This study aimed to develop hybrid composite joints between epoxy composites and PEEK/PPS composites with structural integrity. The surface of the PEEK/PPS composite was treated by a high-power UV-irradiation technique for 6 s, and then co-bonded with epoxy composite with and without an adhesive layer at the interface. The experimental results of the mode-II and mix mode-I/II fracture tests revealed that the addition of an adhesive layer at the joining interface of the hybrid composite joints was necessary to obtain high levels of fracture toughness. For example, the mode-II and mix mode-I/II fracture energies of the adhesively bonded epoxy/PEEK joints were 3.68 kJ/m^2 and 1.73 kJ/m^2, respectively, that were 37% and 116% higher than their counterparts without adhesives. These observations, together with the results of the lap-shear tests and the mode-I fracture tests that were reported in previous work [15] demonstrated that the hybrid joints bonded by adhesives possessed excellent structural performance under different critical loading conditions. Importantly, for the hybrid joints bonded by adhesives, a cohesive failure within the adhesive layer was observed in all the cases. This indicated that the application of the rapid UV-treatment to the surfaces of the PEEK and PPS composites had effectively improved their intrinsically poor adhesion with the adhesive, and subsequently prevented adhesive failure of the hybrid composite joints. Overall, by a combining usage of a co-bonding process and a high-power UV-irradiation surface treatment technique, hybrid adhesive joints between thermoset composites and advanced thermoplastic composites with high structural integrity were obtained.

CRediT authorship contribution statement

Dong Quan: Conceptualization, Investigation, Writing – original draft. **Guoqun Zhao:** Resources, Methodology, Writing – review & editing. **Guilong Wang:** Resources, Investigation, Writing – review & editing. **René Alderliesten:** Methodology, Writing – review & editing.

Declaration of competing interest

The authors declare that they have no known competing financial interests or personal relationships that could have appeared to influence the work reported in this paper.

Data availability

The raw/processed data required to reproduce these findings cannot be shared at this time as the data also forms part of an ongoing study.

Acknowledgements

The authors would like to acknowledge the financial supports from the key research and development program of Shandong Province (Grant No. 2021ZLGX01). We acknowledge Dr. Brian Deegan (Henkel Ireland Operations & Research Ltd., Ireland) for the valuable technical assistance and discussions. Guilong Wang is grateful to the National Natural Science Foundation of China (NSFC, Grant No. 51875318, 52175341) and Shandong Provincial Key Research and Development Program (Major Scientific and Technological Innovation Project) (Grant No. 2019JZZY020205).

References

[1] Borba N, dos Santos J, Amancio-Filho S. Hydrothermal aging of friction riveted thermoplastic composite joints for aircraft applications. Compos Struct 2021;255:112871. http://dx.doi.org/10.1016/j.compstruct.2020.112871.

[2] Hu J, Liu A, Zhu S, Zhang H, Wang B, Zheng H, Zhou Z. Novel panel-core connection process and impact behaviors of CF/PEEK thermoplastic composite sandwich structures with truss cores. Compos Struct 2020;251:112659. http://dx.doi.org/10.1016/j.compstruct.2020.112659.

[3] Airbus. https://www.airbus.com/en/newsroom/news/2017-01-wing-of-the-future, Last Accessed 24th December 2021.

[4] Borba NZ, Kotter B, Fiedler B, dos Santos JF, Amancio-Filho ST. Mechanical integrity of friction-riveted joints for aircraft applications. Compos Struct 2020;232:111542. http://dx.doi.org/10.1016/j.compstruct.2019.111542.

[5] Meng L, Wan Y, Ohsawa I, Takahashi J. Effects of geometric parameters on the failure behavior of mechanically fastened chopped carbon fiber tape reinforced thermoplastics. Compos Struct 2019;229:111475. http://dx.doi.org/10.1016/j.compstruct.2019.111475.

[6] Mund M, Lippky K, Blass D, Dilger K. Influence of production based surface topography and release agent amount on bonding properties of CFRP. Compos Struct 2019;216:104–11. http://dx.doi.org/10.1016/j.compstruct.2019.02.026.

[7] Wolter N, Beber VC, Brede M, Koschek K. Adhesively- and hybrid- bonded joining of basalt and carbon fibre reinforced polybenzoxazine-based composites. Compos Struct 2020;236:111800. http://dx.doi.org/10.1016/j.compstruct.2019.111800.

[8] Huang Y, Meng X, Xie Y, Lv Z, Wan L, Cao J, Feng J. Friction spot welding of carbon fiber-reinforced polyetherimide laminate. Compos Struct 2018;189:627–34. http://dx.doi.org/10.1016/j.compstruct.2018.02.004.

[9] Pereira D, Oliveira JP, Santos TG, Miranda RM, Lourenco F, Gumpinger J, Bellarosa R. Aluminium to carbon fibre reinforced polymer tubes joints produced by magnetic pulse welding. Compos Struct 2019;230:111512. http://dx.doi.org/10.1016/j.compstruct.2019.111512.

[10] Pramanik A, Basak AK, Dong Y, Sarker PK, Uddin MS, Littlefair G, Dixit AR, Chattopadhyaya S. Joining of carbon fibre reinforced polymer (CFRP) composites and aluminium alloys - A review. Composites A 2017;101:1–29. http://dx.doi.org/10.1016/j.compositesa.2017.06.007.

[11] Kodokian GKA, Kinloch AJ. Surface pretreatment and adhesion of thermoplastic fibre-composites. J Mater Sci Lett 1988;7(6):625–7. http://dx.doi.org/10.1007/BF01730315.

[12] Kodokian GKA, Kinloch AJ. The adhesive fracture energy of bonded thermoplastic fibre-composites. J Adhes 1989;29(1–4):193–218. http://dx.doi.org/10.1080/00218468908026487.

[13] Gonzalez-Murillo C, Ansell MP. Co-cured in-line joints for natural fibre composites. Compos Sci Technol 2010;70(3):442–9. http://dx.doi.org/10.1016/j.compscitech.2009.11.017.

[14] Mohan J, Ivankovic A, Murphy N. Mode I fracture toughness of co-cured and secondary bonded composite joints. Int J Adhes Adhes 2014;51:13–22. http://dx.doi.org/10.1016/j.ijadhadh.2014.02.008.

[15] Quan D, Alderliesten R, Dransfeld C, Tsakoniatis I, Benedictus R. Co-cure joining of epoxy composites with rapidly UV-irradiated PEEK and PPS composites to achieve high structural integrity. Compos Struct 2020;251:112595. http://dx.doi.org/10.1016/j.compstruct.2020.112595.

[16] Silverstein MS, Breuer O. Relationship between surface properties and adhesion for etched ultra-high-molecular-weight polyethylene fibers. Compos Sci Technol 1993;48(1):151–7. http://dx.doi.org/10.1016/0266-3538(93)90131-Y.

[17] Tiwari S, Bijwe J, Panier S. Tribological studies on polyetherimide composites based on carbon fabric with optimized oxidation treatment. Wear 2011;271(9):2252–60. http://dx.doi.org/10.1016/j.wear.2010.11.052.

[18] Popelka A, Krupa I, Novak I, Al-Maadeed MASA, Ouederni M. Improvement of aluminum/polyethylene adhesion through corona discharge. J Phys D: Appl Phys 2016;50(3):035204. http://dx.doi.org/10.1088/1361-6463/50/3/035204.

[19] Popelka A, Novák I, Al-Maadeed MAS, Ouederni M, Krupa I. Effect of corona treatment on adhesion enhancement of LLDPE. Surf Coat Technol 2018;335:118–25. http://dx.doi.org/10.1016/j.surfcoat.2017.12.018.

[20] Zhang W, Cao Y, Yang P, Chen M, Zhou X. Manufacturing and interfacial bonding behavior of plasma-treated-carbon fiber reinforced veneer-based composites. Compos Struct 2019;226:111203. http://dx.doi.org/10.1016/j.compstruct.2019.111203.

[21] Borooj MB, Shoushtari AM, Haji A, Sabet EN. Optimization of plasma treatment variables for the improvement of carbon fibres/epoxy composite performance by response surface methodology. Compos Sci Technol 2016;128:215–21. http://dx.doi.org/10.1016/j.compscitech.2016.03.020.

[22] Farris S, Pozzoli S, Biagioni P, Duo L, Mancinelli S, Piergiovanni L. The fundamentals of flame treatment for the surface activation of polyolefin polymers - A review. Polymer 2010;51(16):3591–605. http://dx.doi.org/10.1016/j.polymer.2010.05.036.

[23] Williams DF, Abel M-L, Grant E, Hrachova J, Watts JF. Flame treatment of polypropylene: A study by electron and ion spectroscopies. Int J Adhes Adhes 2015;63:26–33. http://dx.doi.org/10.1016/j.ijadhadh.2015.07.009.

[24] ASTM Standard D7905/D7905M. Standard Test Method for Determination of the Mode II Interlaminar Fracture Toughness of Unidirectional Fiber-Reinforced Polymer Matrix Composites. ASTM International; 2019.

[25] Blackman BRK, Kinloch AJ. Fracture tests for structural adhesive joints. In: Moore D, Pavan A, Williams J, editors. Fracture Mechanics Testing Methods for Polymers, Adhesives and Composites. Amsterdam: Elsevier Science; 2001, p. 225–70.

[26] BS 7991:2001. Determination of the Mode I Adhesive Fracture Energy, GIC, of Structural Adhesives Using the Double Cantilever Beam (DCB) and Tapered Double Cantilever Beam (TDCB) Specimens. British Standard Institute; 2001.

[27] ISO 15114:2014. Fibre-Reinforced Plastic Composites-Determination of Mode II Fracture Resistance for Unidirectionally Reinforced Materials Using the Calibrated End-Loaded Split (C-ELS) Test and an Effective Crack Length Approach. International Organization for Standardization; 2014.

[28] Quan D, Bologna F, Scarselli G, Ivanković A, Murphy N. Mode-II fracture behaviour of aerospace-grade carbon fibre/epoxy composites interleaved with thermoplastic veils. Compos Sci Technol 2020;191:108065. http://dx.doi.org/10.1016/j.compscitech.2020.108065.

[29] Palazzetti R, Zucchelli A. Electrospun nanofibers as reinforcement for composite laminates materials - A review. Compos Struct 2017;182:711–27. http://dx.doi.org/10.1016/j.compstruct.2017.09.021.